ISSN 0023-1584, Kinetics and Catalysis, 2010, Vol. 51, No. 2, pp. 299–311. © Pleiades Publishing, Ltd., 2010.
Original Russian Text © A.A. Firsova, T.I. Khomenko, O.N. Sil'chenkova, V.N. Korchak, 2010, published in Kinetika i Kataliz, 2010, Vol. 51, No. 2, pp. 317–329.

Oxidation of Carbon Monoxide in the Presence of Hydrogen on the CuO, CoO, and Fe_2O_3 Oxides Supported on ZrO_2

A. A. Firsova, T. I. Khomenko, O. N. Sil'chenkova, and V. N. Korchak

Semenov Institute of Chemical Physics, Russian Academy of Sciences, Moscow, 119991 Russia

e-mail: korchak@ctnter.chph.ras.ru

Received December 25, 2008

Abstract—The catalytic activity of the CuO/ZrO_2, CoO/ZrO_2, Fe_2O_3/ZrO_2, and $CuO/(CoO, Fe_2O_3)/ZrO_2$ systems in the reaction of selective CO oxidation in the presence of hydrogen was studied at 20–450°C over the oxide concentration range of 2.5–10 wt % on the surface of ZrO_2. The conversion of CO on the CoO/ZrO_2 systems was almost independent of the concentration of CoO: 88 or 90% for 2.5 or 10% CoO, respectively. TPR data allowed us to relate the catalytic activity of CoO/ZrO_2 to Co–O–Zr clusters, the amount of which was almost constant over the test range of CoO concentrations. The conversion of CO on 2.5% CuO/ZrO_2 was 32% (190°C) or 62–66% on 5–10% CuO/ZrO_2 (170°C). According to TPR data, clusters like Cu–O–Zr occurred on the surface of ZrO_2, and the amount of these clusters reached a maximum upon supporting 5% CuO. The catalytic properties of 5% CuO/5% CoO/ZrO_2 and 5% CoO/5% CuO/ZrO_2 samples were identical to those of 5% CuO/ZrO_2 samples. It is likely that the formation of active reaction sites upon consecutively supporting the oxides occurred on the same surface sites of ZrO_2. In this case, Co and Cu oxides competed for cluster formation, and the copper cation can displace the cobalt cation from the formed clusters. The Fe_2O_3 samples were inactive; a maximum conversion of 34% (290°C) was observed on 10% Fe_2O_3/ZrO_2. The catalytic properties of $CuO/Fe_2O_3/ZrO_2$ were also identical to those of CuO/ZrO_2, and they depended on the presence of Cu–O–Zr clusters on the surface.

DOI: 10.1134/S0023158410020205

INTRODUCTION

The development of environmentally appropriate energy sources using hydrogen as the fuel is a problem of increasing current interest. New types of fuel cells have been developed to replace internal combustion engines; however, they can efficiently operate only with the use of high-purity hydrogen. Commercially produced hydrogen contains 0.5–2 vol % CO in addition to CO_2 in mixtures [1, 2]. For the use of this hydrogen in cells with platinum electrodes or bimetallic catalysts like PtRu, the concentration of the CO impurity should be decreased below 10 or 100 ppm, respectively [3–5]. The low-temperature catalytic oxidation of CO in an atmosphere of hydrogen with oxygen or air is most promising for the removal of CO impurities from the mixtures. Various supported catalytic systems with the use of Pt, Ru, Pd, and Au noble metals [3, 6–9] or Co [10–13] and Cu oxides [14–19] as active components were proposed. Among the test systems, the CuO/CeO_2 catalysts were found the most active and selective; this was explained by the strong Cu–O–Ce interaction on the catalyst surface and, consequently, the formation of highly active oxygen, which is capable of oxidizing CO at 100–160°C. It was found [19] that CO was adsorbed on the surface of oxidized catalysts at $CuO–CeO_2$ clusters with the formation of $CO–Cu^+$ carbonyls and oxidized by the oxygen of these clusters.

A study of the oxidation of CO in mixtures with an excess of oxygen on catalytic systems containing transition metal (Fe, Co, and Ni) oxides in addition to CuO on the surface of CeO_2 [20, 21] demonstrated that, upon the introduction of these additives, which are less active than CuO in this reaction, the conversion of CO increased and the reaction temperature range broadened in the region of a maximum conversion. This is a very important factor for the stable operation of a catalyst under exothermic reaction conditions. Firsova et al. [21] found that new clusters like Cu–(Fe, Co, Ni)–Ce–O were formed on the surface in addition to Cu–O–Ce clusters. In this case, the maximum conversion of CO (>99%) on catalysts with various concentrations of copper oxide, which is responsible for catalyst activity [19] (5% CuO/CeO_2 and 2.5% CuO/2.5% $(Fe_2O_3, CoO, NiO)/CeO_2$), was reached at the same temperature; this suggests close binding energies of oxygen in clusters with different cationic compositions. It is likely that the oxidation of CO occurred at the same cluster fragment, most likely, at $Cu^{2+}–O^{2-}–Ce^{4+}$, which was also present as a constituent of new clusters, whereas the cations of Fe, Co, and Ni, which actively participate in redox processes, facilitated oxygen transfer to these active sites.

In this work, we continued the study of the oxidation of CO in the presence of hydrogen on supported oxide systems. It is well known [22] that the conver-

Table 1. XRD data

Sample	Phase composition*
ZrO_2 (initial)	ZrO_2(M + T**)
5% CuO/ZrO_2	ZrO_2(M + T**)
10% CuO/ZrO_2	ZrO_2(M + T**) + CuO
5% CoO/ZrO_2	ZrO_2(M + T**) + Co_3O_4
10% CoO/ZrO_2	ZrO_2(M + T**) + Co_3O_4
5% CuO/5% CoO/ZrO_2	ZrO_2(M + T**) + (Co_3O_4)**
5% CuO/10% CoO/ZrO_2	ZrO_2(M + T**) + Co_3O_4 + $(Co_{1-x}Cu_xCo_2O_4)$**
10% CoO/5% CuO/ZrO_2	ZrO_2(M + T**) + Co_3O_4 + $(Co_{1-x}Cu_xCo_2O_4)$**
5% Fe_2O_3/ZrO_2	ZrO_2(M + T**)
10% Fe_2O_3/ZrO_2	ZrO_2(M + T**)
5% CuO/10% Fe_2O_3/ZrO_2	ZrO_2(M + T**)

*M and T refer to monoclinic and tetragonal modifications, respectively.

**Traces.

sion of CO into CO_2 in the absence of hydrogen on copper oxide supported onto ZrO_2 was as high as 100%. However, in the oxidation of CO in mixtures with hydrogen [23], the activity of CuO/ZrO_2 and $CuO/(CeO_2–ZrO_2)$ catalysts was lower than that of CuO/CeO_2. In order to obtain new data on the structure of active reaction sites and the role of a support in the formation of these sites for the development of highly efficient catalysts, we studied CuO/ZrO_2, CoO/ZrO_2, Fe_2O_3/ZrO_2, and the $CuO/(CoO, Fe_2O_3)/ZrO_2$ mixed oxide systems.

EXPERIMENTAL

Zirconium dioxide ($S_{sp} = 58$ m^2/g) was prepared by the thermal decomposition of the zirconium(IV) oxynitrate $ZrO(NO_3)_2 \cdot 6H_2O$ in air successively at 300°C for 2 h and at 500°C for 3 h. The specific surface area of catalysts was measured using the BET method based on the low-temperature adsorption of argon.

The CuO/ZrO_2, CoO/ZrO_2, and Fe_2O_3/ZrO_2 catalysts were prepared by the impregnation of zirconium dioxide with the solutions of copper, cobalt, and iron nitrates, respectively. Thereafter, the samples were dried at 120 and 200°C and then calcined at 500°C for 2 h. The CuO contents of the samples were 2.5, 5.0, and 10.0 wt %, respectively.

The samples of $CuO/(CoO$ or $Fe_2O_3)/ZrO_2$ were prepared by supporting CuO onto the CoO/ZrO_2 or Fe_2O_3/ZrO_2 catalysts, which were impregnated with a copper nitrate solution, dried at 200°C, and calcined at 500°C for 2 h. The $CuO/(CoO$ or $Fe_2O_3)/ZrO_2$ systems thus prepared contained 5.0 wt % CuO and 5.0 or 10.0 wt % CoO and Fe_2O_3.

The $CoO/CuO/ZrO_2$ catalysts were prepared by supporting CoO from a solution of cobalt nitrate onto CuO/ZrO_2 followed by drying at 200°C and calcination at 500°C; the samples contained 2.5 and 5.0 wt % CuO and 5.0 or 10.0 wt % CoO.

Note that the specified concentrations of supported components correspond to those calculated from the stoichiometry of the decomposition of corresponding metal nitrates.

The synthesized catalysts were studied by XRD on a DRON-3M instrument, which was calibrated with the use of SiO_2 (α-quartz) powder (CuK_α radiation; graphite monochromator; scanning in 0.02° steps over the angle range of $2\theta = 8°–70°$).

The reaction of CO oxidation with oxygen in an excess of hydrogen was performed in a flow-type system. The reaction mixture containing 98 vol % H_2, 1 vol % CO, and 1 vol % O_2 was passed through a quartz tube reactor (3 mm in diameter) with a catalyst (20 mg; size fraction of 0.25–0.50 mm) at a flow rate of 40 ml/min. The tip of a thermocouple was arranged outside the reactor at a level of the center of the catalyst bed, whose height was 2.0–2.5 mm.

The reaction products were analyzed by chromatography using two columns packed with molecular sieve NaX (13 Å) and Porapak QS and thermal-conductivity detectors.

The TPR of the catalysts was performed in a flow of a 6% H_2/Ar mixture at a rate of 100 ml/min with a thermal-conductivity detector. Heating over the temperature range of 20–650°C was performed at a rate of 12 K/min. Before the experiments, the samples (100 mg) were calcined at 500°C in flowing air for 1 h. The amount of absorbed hydrogen was determined from TPR peak areas to within ~10%.

The surface states of the support and samples with supported metal oxides were studied by IR spectroscopy using CO as a test molecule.

The IR transmission spectra were measured using a Perkin Elmer Spectrum RX 1 FT IR System spectrometer. The samples were pressed in pellets (S = 2 cm^2) at $P = 5000$ kg/cm^2, conditioned in a flow of N_2 at 400°C for 15 min, and then cooled to room temperature; a mixture of 1% CO/N_2 was passed at a flow rate of 50 cm^3/min, and the IR spectra were recorded while increasing the temperature in steps.

RESULTS

Catalyst Characterization by XRD

Table 1 summarizes the XRD data. The initial ZrO_2 mainly occurred in a monoclinic modification (M phase). In addition, low-intensity reflections due to a tetragonal modification (T phase), whose concentration was no higher than ~10%, were detected in the diffraction pattern. An analysis of spectral lines using the Debye–Scherrer formula allowed us to determine the particle size of zirconium dioxide; it was ~30 nm.

The effect of supported Cu, Co, and Fe oxides on the line width was not found; the phase composition of the ZrO_2 support remained unchanged, and the M and T phases were present in all of the supported samples.

New phases were not detected in the 5% CuO/ZrO_2 sample using XRD analysis; this can be due to the amorphous or dispersed state of CuO particles on the surface. As the copper oxide content of the sample was increased to 10%, the diffraction pattern exhibited reflections due to crystalline of CuO. The Co_3O_4 phase was formed in CoO/ZrO_2 samples upon supporting cobalt oxide. This phase was present in all of the $CuO/CoO/ZrO_2$ mixed systems; however, we failed to clearly detect CuO in them using XRD analysis. Moreover, low-intensity reflections suggesting the formation of $Co_{1-x}Cu_xCo_2O_4$ spinel appeared in the diffraction patterns of the $CuO/CoO/ZrO_2$ systems.

Iron oxide phases were not detected in the diffraction patterns of samples containing 5 and 10% Fe_2O_3; this can also be due to an either amorphous or dispersed state of Fe_2O_3 particles on the surface of ZrO_2. The same diffraction patterns were also obtained for the 5% CuO/10% Fe_2O_3/ZrO_2 sample; the CuO phase was also not detected.

Catalytic Activity of ZrO_2, CuO/ZrO_2, CoO/ZrO_2, Fe_2O_3/ZrO_2, and $CuO/(CoO$ or $Fe_2O_3)/ZrO_2$ in CO Oxidation with Oxygen in Excess Hydrogen

The oxidation of CO on ZrO_2, CuO/ZrO_2, CoO/ZrO_2, Fe_2O_3/ZrO_2, and $CuO/(CoO$ or $Fe_2O_3)/ZrO_2$ samples was performed at 20–400°C. Zirconium dioxide is inactive in this temperature range, and the oxidation of CO was not observed.

The catalytic activity of 2.5–10% CuO/ZrO_2 samples depends on the amount of CuO on the surface. In this case, the maximum conversion of CO upon supporting CuO was 32 (190°C), 62 (170°C), or 66% (170°C) for 2.5, 5, or 10 wt % CuO (the maximum conversion temperature T_{max} is specified in parentheses), respectively (see Fig. 1a). An increase in the amount of supported copper oxide from 2.5 to 5% caused an increase in the conversion of CO by a factor of 2 and the occurrence of the reactions in the region of lower temperatures; however, as the concentration of CuO was further increased to 10%, the catalytic activity remained almost unchanged (Fig. 1a, curves *2* and *3*).

The process selectivity for oxygen on CuO/ZrO_2 samples also changed depending on the amount of copper oxide supported onto the surface (Fig. 1b). The selectivity of the 2.5% CuO/ZrO_2 falls in the range of 0–40% to reach a maximum at 190–200°C (Fig. 1b, curve *1*). The maximum selectivity on the 10% CuO/ZrO_2 catalyst (Fig. 1b, curve *3*) was somewhat higher (about 50% at 150°C), and 100% selectivity in the region of low temperatures was observed only on the 5% CuO/ZrO_2 sample (Fig. 1b, curve *2*). At higher

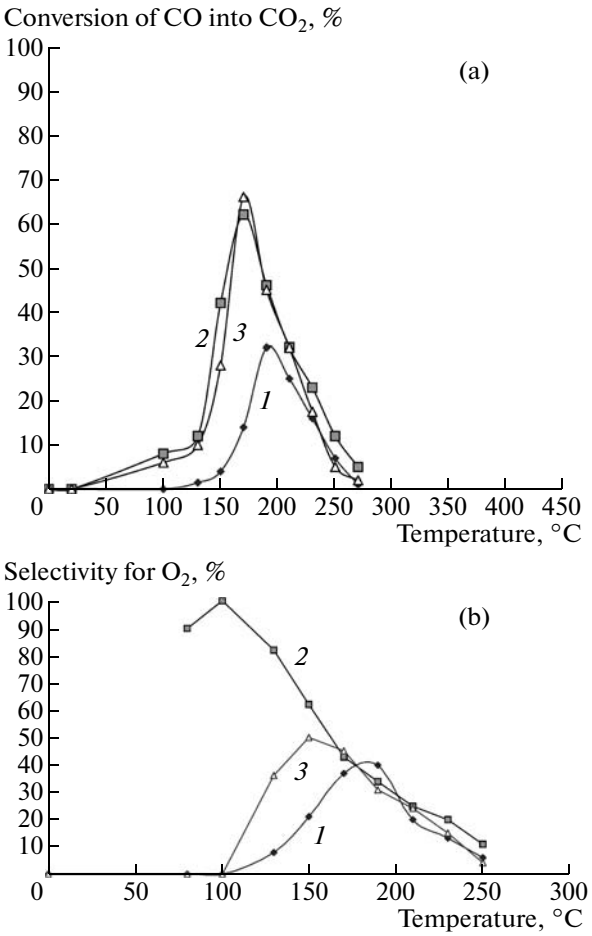

Fig. 1. (a) The conversion of CO into CO_2 and (b) the process selectivity for oxygen on the (*1*) 2.5% CuO/ZrO_2, (*2*) 5% CuO/ZrO_2, and (*3*) 10% CuO/ZrO_2 catalysts.

temperatures (170–250°C), the selectivity was almost the same on all of the CuO/ZrO_2 samples.

The CoO/ZrO_2 catalysts were found to be more active than CuO/ZrO_2. The conversion of CO into CO_2 was 90% (T_{max} = 225°C) on the 10% CoO/ZrO_2 sample, and it depended only slightly on the amount of supported CoO: it was 88% on 2.5% CoO/ZrO_2 at T_{max} = 250°C (see Fig. 2a, curves *1*–*3*). Above 300°C, the reaction of CO hydrogenation comes into play, and methane appeared in the products. The conversion of CO into CH_4 increased with the surface concentration of CoO to reach 4% (390°C) upon supporting 2.5% CoO or 7.5 and 17% on 5% CoO/ZrO_2 and 10% CoO/ZrO_2, respectively. Note that, as the concentration of CoO was increased, the onset temperature of CO hydrogenation decreased from 330 to 290°C and the T_{max} of CO conversion into CO_2 decreased from 250 to 225°C.

The reaction selectivity for oxygen on CoO/ZrO_2 samples was higher than that on CuO/ZrO_2 (see Fig. 2b): 60–82% at 130–250°C on 2.5% CoO/ZrO_2 (curve *1*) or 25–62% at 150–275°C on 10% CoO/ZrO_2

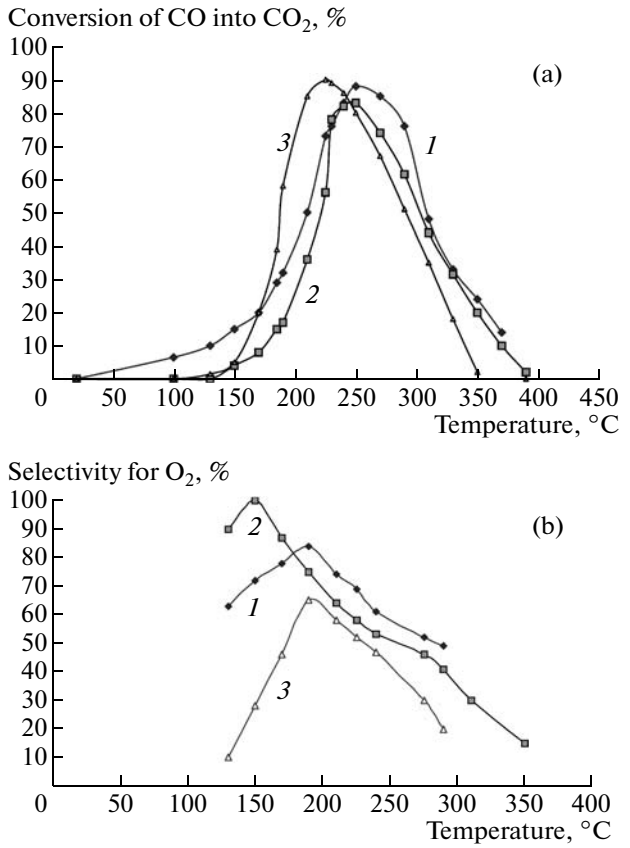

Fig. 2. (a) The conversion of CO into CO_2 and (b) the process selectivity for oxygen on the (*1*) 2.5% CoO/ZrO_2, (*2*) 5% CoO/ZrO_2, and (*3*) 10% CoO/ZrO_2 catalysts.

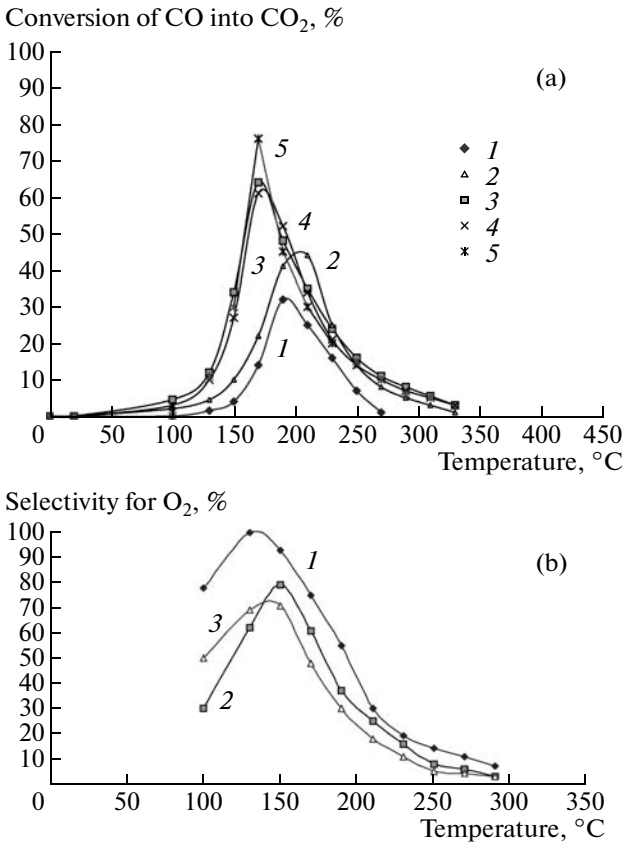

Fig. 3. (a) The conversion of CO into CO_2 on the (*1*) 2.5% CuO/ZrO_2, (*2*) 5% $CoO/2.5\%$ CuO/ZrO_2, (*3*) 5% $CoO/5\%$ CuO/ZrO_2, (*4*) 5% $CuO/5\%$ CoO/ZrO_2, and (*5*) 10% $CoO/5\%$ CuO/ZrO_2 catalysts and (b) the process selectivity for oxygen on the (*1*) 5% $CoO/2.5\%$ CuO/ZrO_2, (*2*) 5% $CoO/5\%$ CuO/ZrO_2, and (*3*) 10% $CoO/5\%$ CuO/ZrO_2 catalysts.

(curve *3*), and it reached 100% at 150°C on the 5% CoO/ZrO_2 sample, as well as on 5% CuO/ZrO_2. In the region of high temperatures (250–350°C), the highest selectivity (58–48%) was observed on the 2.5% CoO/ZrO_2 sample (curve *1*), on which the conversion of CO into CH_4 was minimal, whereas the selectivity was lower (45–18%) on 10% CoO/ZrO_2 at the same temperatures (curve *3*).

Figure 3a shows the catalytic activity of samples prepared by the successive supporting of CuO and CoO onto the surface of ZrO_2. The conversion of CO on the 5% $CoO/2.5\%$ CuO/ZrO_2 sample (curve *2*) increased, as compared with that on 2.5% CuO/ZrO_2 (curve *1*), from 32 to 44% with a T_{max} shift from 190 to 210°C; however, it did not reach the conversion of CO on 5% CoO/ZrO_2. The supporting of 5% CoO onto the 5% CuO/ZrO_2 catalyst (curve *3*) had almost no effect on the catalytic activity: the conversion of CO on the 5% $CoO/5\%$ CuO/ZrO_2 sample was the same as that on 5% CuO/ZrO_2 (curve *4*); however, the conversion of CO on the 10% $CoO/5\%$ CuO/ZrO_2 catalyst (curve *5*) increased to 76% ($T_{max} = 170$°C).

Note that an increase in the conversion of CO on the last sample occurred because of the presence of cobalt oxide in the $CoO/CuO/ZrO_2$ system; however, $T_{max} = 170$°C was much lower than that on CoO/ZrO_2 ($T_{max} = 225$°C), and the same value of T_{max} was observed only on CuO/ZrO_2 samples.

The activity of catalysts prepared by supporting 5% CuO on 5% CoO/ZrO_2 was similar to that of 5% $CoO/5\%$ CuO/ZrO_2 (curve *5*); that is, the order of supporting cobalt and copper oxides onto ZrO_2 had no effect on their catalytic properties.

The reaction selectivity for oxygen on the $CoO/CuO/ZrO_2$ mixed oxide systems was higher than that on individual CuO/ZrO_2 or CoO/ZrO_2 (see Fig. 3b). The maximum 100% selectivity was observed at 130–150°C on the 5% $CoO/2.5\%$ CuO/ZrO_2 sample (curve *1*), whereas the maximum selectivity was 79 or 71% at 150°C on the 5% $CoO/5\%$ CuO/ZrO_2 (curve *2*) or 10% $CoO/5\%$ CuO/ZrO_2 sample (curve *3*), respectively. In the region of high temperatures (>250°C), the selectivity was much higher than that on the CoO/ZrO_2 systems; this was likely due to a shift in the temperature range of the occurrence of CO oxidation to CO_2 and CO conversion into CH_4 toward

low temperatures. This selectivity was comparable with the selectivity on CuO/ZrO_2 samples.

The conversion of CO on the samples prepared by supporting Fe_2O_3 onto ZrO_2 was low: the oxidation of CO began at a temperature of ~200°C; the maximum conversion on the 5% Fe_2O_3/ZrO_2 sample was 20% at 250°C or 34% at 290°C on 10% Fe_2O_3/ZrO_2. The 5% $CuO/5–10\%$ Fe_2O_3/ZrO_2 systems prepared by the successive supporting of iron and copper oxides onto zirconium dioxide exhibited the same activity in CO oxidation as 5% CuO/ZrO_2 regardless of iron oxide content.

TPR Data

ZrO_2. The TPR spectrum of ZrO_2 exhibited a broad low-intensity band of hydrogen uptake with a maximum at 200–300°C. It is well known [24] that ZrO_2 forms several polymorphous modifications, of which a monoclinic (M) species is most thermodynamically stable under normal conditions. Tetragonal (T) and cubic (C) modifications are formed at much higher calcination temperatures (1200–1500 and 2400°C, respectively). However, these phases were also detected in samples calcined at moderate temperatures, and their amount depended on the oxide preparation procedure. It is believed that the presence of various types of defects is due to the formation of these phases. In addition, Kuznetsova and Sadykov [24], found a linear relationship between the specific surface area of samples (S_{sp}) and the amount of the T phase in the M phase. Thus, at $S_{sp} = 55–60$ m^2/g, the concentration of the T phase can be ~10–20%.

The XRD study of ZrO_2 ($S_{sp} = 58$ m^2/g) used in this work showed the presence of small amounts of the T phase in addition to the M phase. According to Kuznetsova and Sadykov [24], this sample should be highly dispersed and have structural distortions and, consequently, defects of various types. Thus, it is believed that small hydrogen uptake was related to the removal of oxygen bound to these defects.

CuO/ZrO_2. The TPR spectra of 2.5 and 5% CuO/ZrO_2 samples (Fig. 4) exhibited an intense broad peak of hydrogen uptake at ~140°C and two low-intensity peaks at higher temperatures (~190 and ~210°C). The ratio between peak intensities at 140 and ~200°C was constant (~0.4). An increase in the concentration of CuO to 10% resulted in a dramatic increase in peak intensities at ~200°C, whereas the low-temperature peak at ~140°C remained almost unchanged. XRD data suggest the formation of a crystalline CuO phase in this sample. The peak at 140°C was likely due to the reduction of copper cations, which strongly interacted with the surface defects of ZrO_2 to form Cu–O–Zr clusters. The second group of peaks at ~200°C was due to the reduction of surface particles of the CuO phase, the amount of which dramatically increased with the concentration of supported copper oxide.

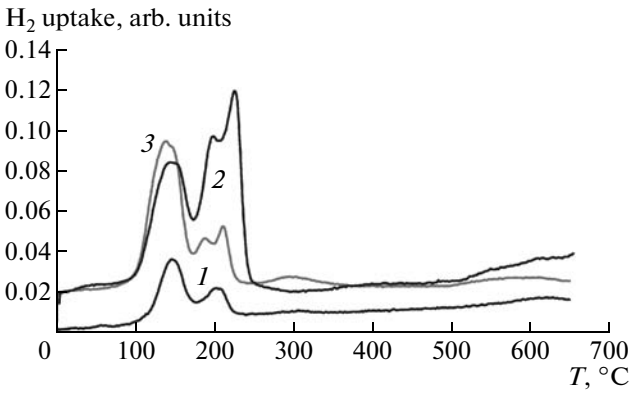

Fig. 4. TPR spectra of CuO/ZrO_2 samples containing (*1*) 2.5, (*2*) 5, and (*3*) 10% CuO.

Dow et al. [25] observed a similar behavior in the reduction of the CuO/ZrO_2 system: two low-intensity TPR peaks (~160–170°C) were ascribed to the removal of oxygen from sites near ZrO_2 defects and at the ZrO_2–CuO interface, whereas an intense peak (~240°C) was attributed to the reduction of bulk oxide. However, the maximum temperatures do not coincide with those observed in this work; this can be due to the history of ZrO_2: Dow et al. [25] used ZrO_2 modified with yttrium and lower concentrations of CuO. This may result in a shift of peaks in the TPR spectrum. A two-peak pattern of this kind was also observed in the CuO/Al_2O_3 system [25, 26]. Thus, upon supporting CuO onto ZrO_2, two types of copper oxide reduction sites were formed: copper oxide particles that strongly interact with the support (it is likely that they form Cu–O–Zr clusters localized near the surface defects of ZrO_2) and the particles of a CuO phase that weakly interacts with the support (its reduction occurred at lower temperatures, as compared with individual CuO). These assumptions are consistent with the results obtained by Labaki et al. [27], who found that copper occurred as isolated cations, clusters, and a CuO phase in CuO/ZrO_2; in this case, the fraction of this phase increased with the concentration of supported copper.

Depending on the CuO content of the sample (2.5–5%), the extent of Cu^{2+} reduction, which was calculated from hydrogen uptake in the range of 140–210°C, changed from 80 to 97% (see Table 2). This was mainly due to an increase in the number of Cu–O–Zr clusters, which are readily reduced at low temperatures, and only a small portion of copper ions, which were present in the 5% CuO/ZrO_2 sample as the surface oxide CuO, was reduced at a higher temperature. The extent of Cu^{2+} reduction in the 10% CuO/ZrO_2 sample decreased to 83.2%, as compared with 5% CuO/ZrO_2 (see Table 2). This decrease in the overall extent of reduction was due to the fact that an additional amount of supported copper oxide, as compared with the 5% CuO/ZrO_2 sample, did almost not

Table 2. TPR data for the ZrO_2, CuO/ZrO_2, CoO/ZrO_2, and Fe_2O_3/ZrO_2 samples

Sample	T_{max}, °C	H_2 uptake $\times 10^4$, mol/g	Extent of transition metal reduction, %	Notes
ZrO_2	~200	–	–	–
2.5% CuO/ZrO_2	149(1)*	1.7(1)*	80.6	Total
	207(2)	0.8(2 + 3)		
	311(3)			
	623(4)			
5% CuO/ZrO_2	142(1)	4.5(1)	97.6	Total
	192(2)	1.6 (peaks 2 + 3)		
	212(3)			
10% CuO/ZrO_2	148	4.3(1)	83.2	Total
	202	6.1 (peaks 2 + 3)		
	227			
	>650			
2.5% CoO/ZrO_2	150	3.9 (total)	86	$Co^{3+} \longrightarrow Co^{2+}$
	285			$Co^{2+} \longrightarrow Co^0$
	515			
5% CuO/ZrO_2	100	11.6 (total)	100	$Co^{3+} \longrightarrow Co^{2+}$
	292			$Co^{2+} \longrightarrow Co^0$, H_2 excess,
	512			2.5×10^{-4} mol/g
10% CuO/ZrO_2	100	21.0 (total)	100	$Co_3O_4 \longrightarrow Co^0$, H_2 excess,
	291			2.4×10^{-4} mol/g
	340			
	403			
	482			
5% Fe_2O_3/ZrO_2	340	3.7	100	$Fe_2O_3 \longrightarrow Fe_3O_4$
			100	$Fe_3O_4 \longrightarrow FeO$
				(1.6×10^{-4} mol Fe^0/g)
10% Fe_2O_3/ZrO_2	342	4.5 (total)	100	$Fe_2O_3 \longrightarrow Fe_3O_4$
	445		58.5	$Fe_3O_4 \longrightarrow FeO$
				(1.8×10^{-4} mol Fe^0/g)
5% CuO/5% CoO/ZrO_2	140	15.2 (total)	99	$Cu^{2+} \longrightarrow Cu^0$,
	192 (shoulder)			$Co_3O_4 \longrightarrow Co^0$
	213			
	304			
5% CuO/10% CoO/ZrO_2	145	27.4 (total)	100	$Cu^{2+} \longrightarrow Cu^0$,
	163			$Co_3O_4 \longrightarrow Co^0$, H_2 excess,
	217			2.5×10^{-4} mol/g
	245			
5% CoO/5% CuO/ZrO_2	152	16.6 (total)	100	$Cu^{2+} \longrightarrow Cu^0$,
	216			$Co_3O_4 \longrightarrow Co^0$, H_2 excess,
	336			1.3×10^{-4} mol/g
5% CoO/2.5% CuO/ZrO_2	161	6.8 (total)	56	For the processes
	221			$Cu^{2+} \longrightarrow Cu^0$,
	339			$Co_3O_4 \longrightarrow Co^0$, $12.2 \times$
	555			10^{-4} mol H_2/g is required
10% CoO/5% CuO/ZrO_2	152	24.1 (total)	100	$Cu^{2+} \longrightarrow Cu^0$,
	225			$Co_3O_4 \longrightarrow Co^0$
	316			
5% CuO/5% Fe_2O_3/ZrO_2	139(1)	7.0 (peaks 1–3)	100(CuO)	Total: $Cu^{2+} \longrightarrow Cu^0$
	154(2)		100(Fe_2O_3)	$Fe_2O_3 \longrightarrow Fe_3O_4$ (100%)
	194 (shoulder 3)			$Fe_3O_4 \longrightarrow FeO$ (52.4%)
	297(4)	1.4 (peaks 4, 5)		(0.3×10^{-4} mol Fe^0/g)
	400(5)			
5% CuO/10% Fe_2O_3/ZrO_2	137 (shoulder 1)	9.8 (peaks 1–3)	100	$Cu^{2+} \longrightarrow Cu^0$,
	148(2)			$Fe_2O_3 \longrightarrow Fe_3O_4$
	196 (shoulder 3)			$Fe_3O_4 \longrightarrow FeO$
	447(4)	4.2(4)	100	(3.1×10^{-4} mol Fe^0/g)

* Peak number in the TPR spectrum.

change the concentration of surface Cu–O–Zr clusters, which are active reaction sites (readily reducible and reoxidizable). This is evident from data given in Table 2: the absorption of hydrogen at 140°C on both of the samples was the same (~4.5×10^{-4} mol/g), and the maximum conversion of CO was the same (62% on 5% CuO/ZrO_2 or 66% on 10% CuO/ZrO_2). As the concentration of copper oxide supported on ZrO_2 was increased from 5 to 10%, a surface phase of CuO was formed. It is likely that this phase was reduced only partially to decrease the overall extent of Cu^{2+} reduction in the 10% CuO/ZrO_2 sample at higher temperatures (>300°C), as evidenced by wide low-intensity peaks of hydrogen uptake (see Fig. 4) in TPR spectra.

CoO/ZrO_2. The TPR spectra of the samples containing 2.5 and 5% CoO are characterized by the occurrence of a low-intensity broad peak due to hydrogen uptake at 100–150°C and peaks at ~290 and ~510°C (Fig. 5, Table 2). The ratio between the areas of the above two peaks is 1 : 3; this allowed us to attribute them to the following processes of the consecutive reduction of Co_3O_4:

$$Co_3O_4 + H_2 = 3CoO + H_2O,$$
$$CoO + 3H_2 = 3Co + 3H_2O.$$

The great temperature interval between the peaks (~200 K), which is uncharacteristic of these processes, has engaged our attention. However, Chernavskii et al. [28] obtained a spectrum of this kind for a sample of cobalt oxide supported onto zirconium oxide with wide pores modified with yttrium oxide. In our case, the shift of both peaks by 100 K toward high temperatures may be due to the stronger interaction of Co_3O_4 with the support (or coarser cobalt oxide particles). By analogy with published data [29], this strong interaction can be the formation of a cobalt zirconate layer on the contact surface of cobalt oxide and the support, the reduction of which occurs at high temperatures.

The TPR spectrum of the sample with 10% CoO contains the same peaks as the spectra of samples with lower CoO contents; however, the intensity of these peaks is higher. Moreover, intensive hydrogen consumption was observed at 290–510°C; this suggests the occurrence of other cobalt oxide states. The presence of only Co_3O_4 in the 5 and 10% CoO/ZrO_2 samples was detected by XRD analysis. Thus, it is believed that the observed hydrogen uptake was due to the reduction of the Co_3O_4 phase arranged at various surface sites of the support (for example, in pores and on the geometrical surface).

Based on the above data, the degrees of cobalt reduction from Co_3O_4 to Co^0 (~300–500°C) were ~43, 60, and 91% for samples containing 2.5, 5, and 10% CoO, respectively. However, the total amount of hydrogen corresponding to the area under TPR curves was much greater. It is evident that CoO in another form occurred on the surface of ZrO_2 in addition to the Co_3O_4 phase. The reduction of this cobalt oxide corresponds to hydrogen uptake in the temperature

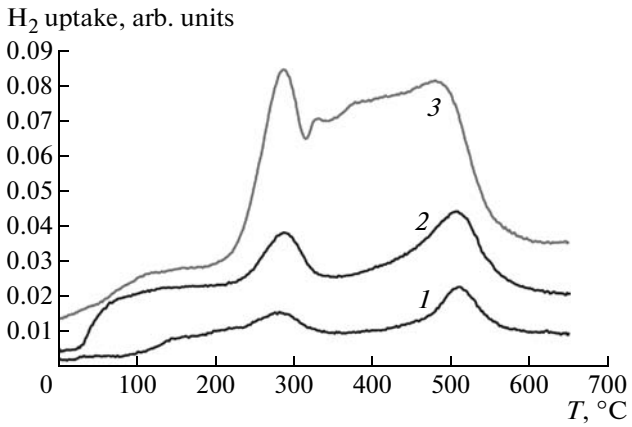

Fig. 5. TPR spectra of CoO/ZrO_2 samples containing (*1*) 2.5, (*2*) 5, and (*3*) 10% CoO.

range of 100–220°C. The amounts of supported CoO, which is reduced at 100–220°C, in all of the samples can be evaluated from the difference between the total amount of absorbed hydrogen and that required for the reduction of Co_3O_4 to Co^0 (~300–500°C). These amounts were ~1.8×10^{-4} mol CoO/g. It is likely that this fraction of cobalt ions was adsorbed at zirconium oxide defects with the formation of Co–O–Zr clusters, as it was observed with copper oxide.

The amount of H_2 absorbed upon the TPR of 5% CoO/ZrO_2 and 10% CoO/ZrO_2 samples was greater than that required for the 100% reduction of cobalt. According to published data, this can be due to the interaction of hydrogen with superstoichiometric oxygen formed in the sample upon the decomposition of cobalt nitrate [28].

$CuO/CoO/ZrO_2$. Figure 6 shows the TPR spectra of samples prepared by supporting CuO onto the surface of 5 and 10% CoO/ZrO_2 catalysts. These spectra suggest the interaction of CuO and CoO oxides: the shape of the spectrum of either of the oxides changed, and the temperature of CoO reduction decreased. However, the intensity and position of the first peak due to CuO reduction (140°C) in the TPR spectrum of the $CuO/CoO/ZrO_2$ system remained almost unchanged (see Fig. 6), as compared with the CuO/ZrO_2 sample. Consequently, even if CoO was initially supported and then CuO was supported, copper oxide partially occupied the same surface sites at which Cu–O–Zr surface clusters were likely formed. At the same time, the hydrogen uptake at ~200°C—the reduction region of the particles of a copper oxide phase bound to the support—increased. The intensity of hydrogen uptake in the high-temperature region of CoO reduction considerably decreased. It is likely that supported bulk CuO and Co_3O_4 oxides interacted on the surface of ZrO_2. A similar behavior of the interaction of oxides (unsupported) was observed by Fierro et al. [30], who used TPR and XPS techniques to demonstrate that the calcination of an oxide mixture at

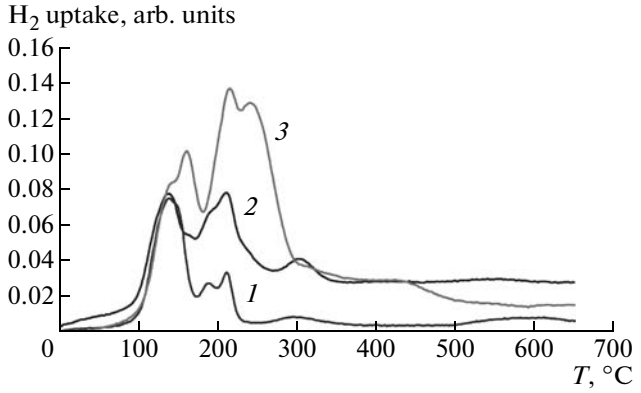

Fig. 6. TPR spectra of (*1*) 5% CuO/ZrO_2, (*2*) 5% CuO/5% CoO/ZrO_2, and (*3*) 5% CuO/10% CoO/ZrO_2 samples.

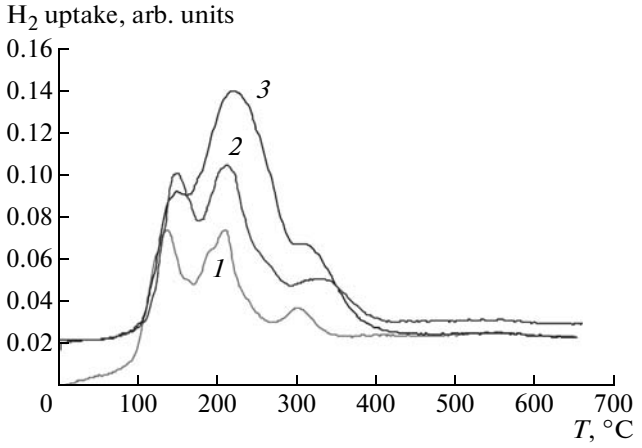

Fig. 7. Effect of the order of supporting oxides on their reduction: (*1*) 5% CuO/5% CoO/ZrO_2, (*2*) 5% CoO/5% CuO/ZrO_2, and (*3*) 10% CoO/5% CuO/ZrO_2.

$T = 450$°C in air resulted in the formation of Co_3O_4 and $Co_{1-x}Cu_xCo_2O_4$ spinel, where x depends on the ratio between the oxides. The reduction of such compounds occurs in two steps: initially, Co^{3+} and Cu^{2+} are reduced to CO^{2+} and Cu^0, respectively, and then CO^{2+} is reduced to Co^0. The XRD data for $CuO/CoO/ZrO_2$ samples (see Table 1) support the formation of $Co_{1-x}Cu_xCo_2O_4$ spinel on the surface of ZrO_2, and a great number of TPR peaks (Fig. 6) in the region of 150–250°C was due to the stepwise reduction of $Co_{1-x}Cu_xCo_2O_4$ and Co_3O_4 unbound to the supported copper oxide.

To understand the effect of the order of supporting copper and cobalt oxides onto the surface of ZrO_2 on the interaction of these oxides, we studied the reduction of $CoO/CuO/ZrO_2$ samples with hydrogen and compared the resulting TPR spectra with data for $CuO/CoO/ZrO_2$ samples (Fig. 7, spectra *1–3*). In the TPR spectrum of the sample prepared by supporting CoO onto the surface of CuO/ZrO_2 (spectra *2, 3*), the maximum temperature of the first peak corresponding to the reduction of Cu–O–Zr was higher by ~10 K. The position of the second peak (corresponding to the reduction of bulk copper and cobalt phases bound to the support) remained unchanged. This fact suggests the formation of the same surface compound regardless of the order of supporting CuO and CoO oxides onto ZrO_2.

As the amount of CoO was increased to 10%, the peak at ~220°C became predominant; this fact suggests that a large portion of cobalt oxide was reduced in this temperature region (with consideration for 100% oxide reduction).

Fe_2O_3/ZrO_2 and $CuO/Fe_2O_3/ZrO_2$. From the TPR spectra of Fe_2O_3/ZrO_2 (maximums at ~340 and 445°C), it follows (see Table 2) that the amount of absorbed hydrogen was sufficient for the sequential 100% reduction $Fe_2O_3 \longrightarrow Fe_3O_4 \longrightarrow FeO$ and to Fe^0 in the 9.5% sample. Because FeO is unstable under ordinary conditions, it disproportionates (with no hydrogen uptake) to Fe_3O_4 and Fe^0 [31]; therefore, the sample additionally contained 1.6×10^{-4} mol Fe^0/g. The occurrence of the second peak of hydrogen uptake at ~445°C supported the assumption on the stepwise reduction of the oxide. However, based on the amount of absorbed hydrogen, we can state 100% reduction to Fe_3O_4 and 58.5% reduction to FeO (in this case, 1.8×10^{-4} mol/g Fe^0 and the same additional amount of Fe_3O_4 were formed). It is likely that coarse particles were formed on the support surface upon supporting iron oxide in a high concentration, and these particles are difficult to reduce.

A comparison between the TPR spectra of the $CuO/Fe_2O_3/ZrO_2$ system containing copper oxide supported after iron oxide (5 and 10%) and CuO/ZrO_2 and Fe_2O_3/ZrO_2 samples led us to a conclusion that the supported oxides strongly interacted with one another. The TPR peak at ~340°C disappeared, and a peak at ~450°C considerably increased (the latter peak was weakly pronounced in the spectra of 5 and 10% Fe_2O_3/ZrO_2 samples). Moreover, absorption increased in the region of copper oxide reduction. The total amount of absorbed hydrogen was sufficient for the 100% reduction of all of the supported oxides to metals.

Adsorption of CO on Copper, Cobalt, and Iron Oxides Supported on ZrO_2 or CeO_2 According to IR Spectroscopic Data

Upon the adsorption of CO on the oxide catalysts, the IR spectra exhibited absorption bands in the following two regions: 1000–1700 (vibrations of carbonate–carboxylate structures) and 2000–2200 cm^{-1} (vibrations of the CO molecule coordinatively bound to a metal cation) [32].

Figure 8 shows the IR spectra of CO adsorbed on ZrO_2 (spectrum *1*) and 5% CuO/ZrO_2 samples (spec-

tra *2–5*). In the spectrum of ZrO_2, absorption bands in the region of 2000–2200 cm^{-1}, which are characteristic of adsorbed carbon monoxide (spectrum *1*), were not detected. Upon supplying a mixture of 1% CO/N_2 onto the 5% CuO/ZrO_2 catalyst, a peak with a maximum at 2100 cm^{-1} appeared even at 40°C (spectrum *2*). The intensity of this peak reached a maximum at T_{max} = 80°C (spectrum *3*), and it decreased as the temperature was further increased (spectra *4*, *5*). According to published data [33–35], an absorption band at 2100 cm^{-1} corresponds to the stretching vibrations of the C–O bond in the CO molecule coordinatively bound to Cu^+ (Cu^+–CO). It is likely that the adsorption of CO occurred at reduced two-dimensional and three-dimensional copper clusters containing Cu^+, which were arranged on the surface of the oxide support. Thus, we can conclude that clusters that can be reduced at low temperatures were formed on the surface of ZrO_2 upon supporting copper oxide. With the use of the molar absorption coefficient of $M^{n+}CO$ complexes, we can evaluate the number of Cu^+ cations on the catalyst surface from the modified Bouguer–Lambert–Beer law

$$\varepsilon = DS_s/N,$$

where ε is the molar absorption coefficient, cm^2/molecule; $D = \log I_0/I$, where I_0 and I are incident and transmitted light intensities at an absorption band maximum; S_s is the cross section of the light flux through the sample, cm^2; and N is the number of adsorbed molecules. The value of ε (Cu^+CO) = 6.7×10^{19} cm^2/molecule was used in the calculations [36]. Table 3 summarizes the results of the calculations.

Upon the adsorption of CO on the surface of the 5% CuO/5% CoO/ZrO_2 catalyst, spectra analogous to spectra *2–4* in Fig. 8 were obtained. The absorption band intensity at 2100 cm^{-1} in this sample at T_{max} = 80°C was almost the same as that in 5% CuO/ZrO_2 (see Table 3).

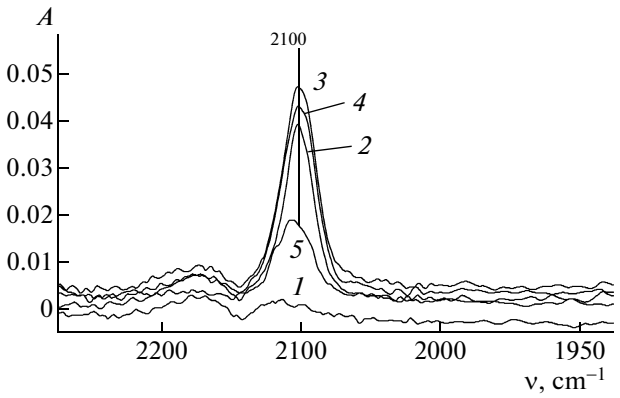

Fig. 8. Difference IR spectra of CO adsorbed on (*1*) ZrO_2 at 40°C and 5% CuO/ZrO_2 samples at (*2*) 40, (*3*) 80, (*4*) 120, or (*5*) 160°C. A spectrum measured in a flow of N_2 was subtracted from the spectrum of a sample measured in a flow of 1% CO/N_2 at each particular temperature.

For comparison, we studied the IR spectra of CO molecules adsorbed on samples that were prepared by supporting copper oxide and cobalt and iron oxides onto cerium dioxide, the catalytic and physicochemical properties of which were described elsewhere [20, 21]. In the spectra of CuO/CeO_2, CuO/(CoO or Fe_2O_3)/CeO_2, and (CoO or Fe_2O_3)/CuO/CeO_2 samples containing copper oxide, an absorption band at 2100 cm^{-1} was observed, whose intensity changed with temperature to pass through a maximum at 120–150°C (see Table 3). By way of example, Fig. 9 shows the IR spectra obtained upon the adsorption of CO on CeO_2 (spectrum *1*), 2.5% CuO/CeO_2 (spectrum *2*, 120°C), 2.5% CuO/2.5% CoO/CeO_2 (spectrum *3*, 150°C), and 2.5% CoO/2.5% CuO/CeO_2 (spectrum *4*, 140°C). Spectra *2–4* correspond to the maximum intensity temperature of the absorption band at 2100 cm^{-1} for each sample. Comparing data in Fig. 9 and Table 3, we can conclude that the greatest amount

Table 3. IR spectroscopic data for CO adsorbed on CeO_2 and ZrO_2 samples containing various oxides

Sample	ν_{max}, cm^{-1}	D	T_{max}, °C	N*, molecule/mg	S_{sp}, m^2/g	N*, molecule/m^2
2.5% CuO/CeO_2	2105	0.2037	120	2.43×10^{16}	65	3.74×10^{17}
6.5% CuO/CeO_2	2105	0.2127	120	2.27×10^{16}	63	3.60×10^{17}
2.5% CuO/2.5% CoO/CeO_2	2103	0.0792	150	7.88×10^{15}	60	1.31×10^{17}
2.5% CoO/2.5% CuO/CeO_2	2102	0.0132	140	1.19×10^{15}	48	2.49×10^{16}
2.5% Fe_2O_3/2.5% CuO/CeO_2	2104	0.1830	120	1.82×10^{16}	50	3.64×10^{17}
2.5% CuO/2.5% Fe_2O_3/CeO_2	2104	0.0163	120	8.25×10^{14}	50	1.65×10^{16}
5% CuO/ZrO_2	2102	0.0375	80	2.24×10^{15}	50	4.48×10^{16}
5% CuO/5% CoO/ZrO_2	2100	0.0193	80	1.75×10^{15}	49	3.56×10^{16}

* The number of adsorbed CO molecules per 1 mg of a pellet or 1 m^2 of its surface area.

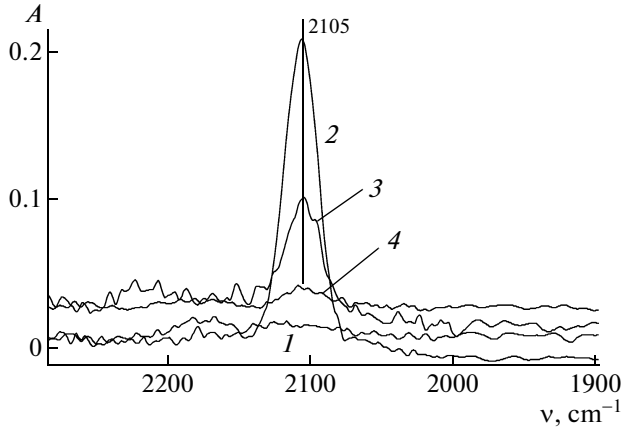

Fig. 9. IR spectra of (*1*) CeO_2 samples at 40°C, (*2*) 2.5% CuO/CeO_2 at 120°C, (*3*) 2.5% CuO/2.5% CoO/CeO_2 at 150°C, and (*4*) 2.5% CoO/2.5% CuO/CeO_2 at 140°C measured in a flow of 1% CO/N_2.

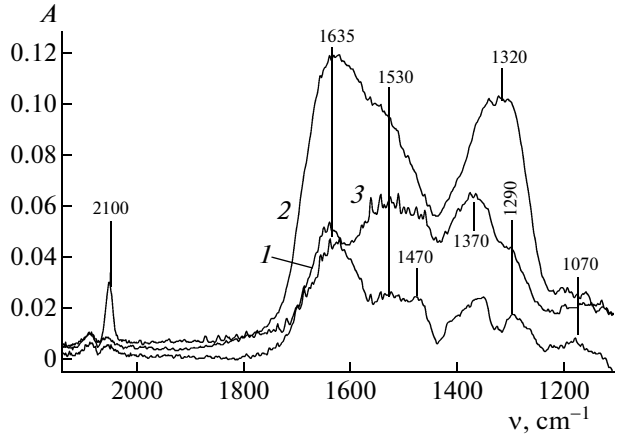

Fig. 10. IR spectra of (*1*) ZrO_2, (*2*) 5% CoO/ZrO_2, and (*3*) 5% CuO/5% CoO/ZrO_2 samples measured in a flow of 1% CO/N_2 at 100°C.

of finely dispersed clusters containing Cu^+ was formed upon supporting only copper oxide onto CeO_2 with the formation of Cu^+–O–Ce sites. In the case of supporting a second oxide (Co or Fe), the amount of Cu^+ cations noticeably decreased, probably, because of the interaction of supported oxides with each other and with the support to form new Cu–Co(Fe)–Ce–O active sites, as found previously [21].

According to IR spectroscopic data (see Table 3), the amount of Cu^+ cations in CuO/ZrO_2 and $CuO/CoO/ZrO_2$ samples was several times smaller than that in the catalysts supported on CeO_2. This fact may be explained by a smaller number of sites for the formation of clusters containing Cu^+ on ZrO_2, as compared with CeO_2.

Absorption bands characteristic of carbonyl complexes bound to the cobalt cation were not observed upon the adsorption of CO on CoO/ZrO_2 and $CoO/CuO/ZrO_2$ samples. However, carbonate–carboxylate structures were formed (1700–1000 cm^{-1}) [37]. Note that carbonate–carboxylate complexes occurred in the IR spectra of almost the entire test catalysts; however, their amount depended on the composition of the catalyst. Figure 10 shows the spectra of (*1*) ZrO_2, (*2*) 5% CoO/ZrO_2, and (*3*) 5% CuO/5% CoO/ZrO_2 samples obtained at 100°C in a flow of 1% CO/N_2. The intensities of absorption bands corresponding to carbonate–carboxylate complexes (1700–1000 cm^{-1}) was much higher for the 5% CoO/ZrO_2 sample (spectrum *2*) than that for pure zirconium dioxide (spectrum *1*). At the same time, upon supporting CuO onto CoO/ZrO_2 (spectrum *3*), the intensities of these absorption bands noticeably decreased, probably, because of a decrease in the amount of Co_3O_4 on the surface of ZrO_2 as a consequence of the interaction with supported copper oxide.

DISCUSSION

The catalytic activity of the CuO/ZrO_2, CoO/ZrO_2, Fe_2O_3/ZrO_2, and $CuO/(CoO, Fe_2O_3)/ZrO_2$ systems and the reaction temperature of CO oxidation with oxygen in the presence of hydrogen depend on the nature of the supported oxides. The results shown in Figs. 1–3 allowed us to present the following order of catalyst activity:

$$(2.5–10)\%CoO/ZrO_2 > (2.5–10)\%CuO/ZrO_2 \sim 5\%CuO/5–10\%(CoO, Fe_2O_3)/ZrO_2 > (5–10)\%Fe_2O_3/ZrO_2 > ZrO_2.$$

The conversion of CO into CO_2 (Fig. 2) was almost independent of the surface concentration of cobalt oxide; it was 88% (T_{max} = 250°C) on 2.5% CoO/ZrO_2 or 90% (T_{max} = 225°C) on 10% CoO/ZrO_2. It is likely that the number of active sites formed on the surface of ZrO_2 upon supporting cobalt oxide was limited. This conclusion is consistent with the results of the TPR of 2.5–10% CoO/ZrO_2 systems; these results indicate that the same amount of CoO (~1.8×10^{-4} mol CoO/g), which is reduced at low temperatures, was present on the surface regardless of the concentration of supported cobalt oxide (2.5–10%). It is likely that this CoO was localized near structure defects on the surface of ZrO_2 (the concentration of these defects was low: ~10–20% of the surface [24]), probably, with the formation of clusters like Co–O–Zr, at which CO was oxidized to CO_2 (200–290°C). At temperatures of >300°C (region of Co_3O_4 reduction to form Co^0), the reaction of CO hydrogenation with the formation of CH_4 occurred. This is consistent with the results obtained in CoO/CeO_2 systems [21] and the generally accepted mechanism of the Fischer–Tropsch process, according to which the dissociative adsorption of CO required for the formation of CH_4 occurs at metal cobalt particles. An increase in the concentration of supported cobalt oxide resulted in an increase in the

amount of the Co_3O_4 phase on the surface of ZrO_2 (Fig. 5) and, consequently, in an increase in Co^0 upon reduction. The conversion of CO into CH_4 (390°C) increased from 4% (2.5% CoO/ZrO_2) to 17% (10% CoO/ZrO_2). Note that the conversion of CO into CH_4 on the CoO/CeO_2 systems [21] was much higher and reached 100% at 400°C, whereas the temperature of Co_3O_4 reduction on the surface of CeO_2 was lower than that on ZrO_2.

The CuO/ZrO_2 catalysts are less active than CoO/ZrO_2: as the amount of supported copper oxide was changed from 2.5 to 5%, the conversion of CO into CO_2 increased by a factor of 2 from 32 to 62%. However, as the concentration of CuO was further increased to 10%, the conversion remained unchanged. The sampled prepared by supporting 5% CoO onto 5% CuO/ZrO_2 exhibited the same catalytic properties as 5% CuO/ZrO_2. This can be explained by the fact that the formation of active sites for CO oxidation with the participation of supported copper or cobalt oxides occurred at the same surface regions of ZrO_2, the number of which is restricted. As demonstrated by TPR data (Fig. 6), Cu–O–Zr clusters occurred in the 5% CoO/5% CuO/ZrO_2 sample; according to catalytic data, the number of these clusters was maximally possible at a 5% CuO content on ZrO_2; that is, there are no free surface sites for the formation of Co–O–Zr clusters.

As noted above, the conversion of CO on the 2.5% CuO/ZrO_2 catalyst was lower than that on 5% CuO/ZrO_2, the number of Cu–O–Zr active sites for CO oxidation on this catalyst was also smaller. Consequently, vacant sites can remain on the surface for the formation of Co–O–Zr clusters. This conclusion was supported by the results obtained in a study of CO oxidation on the 5% CoO/2.5% CuO/ZrO_2 catalyst: the conversion of CO on it increased to 45% (210°C), as compared with 32% (190°C) on 2.5% CuO/ZrO_2. It is likely that, in this case, Co–O–Zr clusters also occurred on the surface of the 5% CoO/2.5% CuO/ZrO_2 catalyst (in addition to Cu–O–Zr clusters). This resulted in an increase in the conversion of CO and a shift in T_{max} toward higher temperatures (210°C) characteristic of CoO/ZrO_2 catalysts. At the same time, the additivity of the catalytic properties of various clusters from this system was not observed. According to XRD data, in the 5% CuO/5% CoO/ZrO_2 or 5% CoO/2.5% CuO/ZrO_2 samples, a portion of supported CoO interacted with surface copper oxide particles to form $Co_{1-x}Cu_xCo_2O_4$ spinel (see Table 1), which is inactive in CO oxidation. The other portion was localized on the surface as a Co_3O_4 phase, the amount of which decreased because of this, as compared with 5% CoO/ZrO_2. In addition to TPR data, this was also supported by the results of IR spectroscopic studies (see Fig. 10), which indicated that the intensity of absorption bands at 1700–1000 cm^{-1} due to carbonate–carboxylate structures formed on Co_3O_4 decreased. An unexpected result was obtained in the 5% CuO/5% CoO/ZrO_2 sample. The conversion of CO into CO_2 and T_{max} on it were the same as those on 5% CuO/ZrO_2; that is, the oxidation of CO most likely occurred at Cu–O–Zr sites, although copper oxide was supported onto the surface of the 5% CoO/ZrO_2 catalyst with the Co–O–Zr oxidation sites. The TPR data (Fig. 6) suggest the occurrence of the Cu–O–Zr clusters in the 5% CuO/5% CoO/ZrO_2 sample. We can conclude that, even in the sequential supporting of cobalt and copper oxides onto the surface of ZrO_2, there was competition for surface regions in which Co–O–Zr and Cu–O–Zr clusters were formed, and the copper cation was capable of partially displacing the cobalt cation from these clusters.

In addition, IR spectroscopic data indicated that the amount of Cu^+–CO centers, which are reaction intermediates, on the surface of 5% CuO/5% CoO/ZrO_2 was almost the same as that on the surface of 5% CuO/ZrO_2 (see Table 3).

The catalytic properties of the $CuO/Fe_2O_3/ZrO_2$ system did not differ from the properties of the CuO/ZrO_2 catalyst. The Fe_2O_3/ZrO_2 sample was inactive in the oxidation of CO, and the presence of iron oxide on the surface of the $CuO/Fe_2O_3/ZrO_2$ sample did not prevent the formation of Cu–O–Zr clusters, as demonstrated for the $CuO/CoO/ZrO_2$ samples. This was supported by TPR data (see Table 2). This did not produce additional active reaction sites, although the supported oxides interacted with each other.

In addition, IR spectroscopic data indicated that the amount of Cu^+–CO centers, which are reaction intermediates, on the surface of 5% CuO/5% CoO/ZrO_2 was almost the same as that on the surface of 5% CuO/ZrO_2 (see Table 3).

The catalytic properties of the $CuO/Fe_2O_3/ZrO_2$ system did not differ from the properties of the CuO/ZrO_2 catalyst. The Fe_2O_3/ZrO_2 sample was inactive in the oxidation of CO, and the presence of iron oxide on the surface of the $CuO/Fe_2O_3/ZrO_2$ sample did not prevent the formation of Cu–O–Zr clusters, as demonstrated for the $CuO/CoO/ZrO_2$ samples. This was supported by TPR data (see Table 2). This did not produce additional active reaction sites, although the supported oxides interacted with each other.

Thus, based on the above experiments, we can hypothesize that Cu–O–Zr and Co–O–Zr clusters, which are active sites for CO oxidation, were formed in defect surface regions upon supporting copper and cobalt oxides onto ZrO_2. However, these defects occupied no more than 10–20% of the surface; this restricted the number of active sites in the catalytic systems. As follows from the TPR data, the amount of hydrogen consumed in the region of the reduction of Cu–O–Zr clusters (4.5×10^{-4} mol/g) for maximally active 5% CuO/ZrO_2 was approximately the same as

that in the region of the reduction of Co–O–Zr (3.9×10^{-4} mol/g) on the surface of 2.5% CoO/ZrO_2.

The process selectivity for oxygen reached 100% on the $CuO(CoO)/ZrO_2$ samples containing no more than 5% Cu or Co oxide (see Figs. 1b and 2b). This also suggests a limited number of active sites on the surface.

The oxidation of CO adsorbed on clusters most likely occurred by oxygen from these clusters, whereas the participation of oxygen from the bulk of the catalyst is unlikely because of a low diffusion coefficient at 100–200°C. In addition, the mobility of lattice oxygen and the rates of the ZrO_2 reduction–reoxidation processes

$$Zr^{3+} + O_2 \rightleftharpoons Zr^{4+} + O_2^-$$

were much lower than those for CeO_2 [38]. This fact may explain higher values of T_{max} on the CuO/ZrO_2 systems (170–190°C), as compared with those on the CuO/CeO_2 catalysts (140–150°C).

Based on the experimental results, we can hypothesize that the oxidation of CO in the presence of hydrogen on the CuO/ZrO_2 and CoO/ZrO_2 samples most likely occurred at Cu–O–Zr or Co–O–Zr clusters analogously to $CuO(CoO)/CeO_2$ catalysts with Cu(Co)–O–Ce oxidation sites. However, the formation of mixed Cu–Co–O–Zr clusters, which might decrease the reaction temperature and increase CO conversion, as in the case of the $CuO/CoO/CeO_2$ systems [21], was not observed in the $CuO/CoO/ZrO_2$ systems upon simultaneously supporting copper and cobalt oxides.

ACKNOWLEDGMENTS

We are grateful to D.P. Shanin for performing the XRD analysis of the samples.

This work was supported by the Russian Foundation for Basic Research (project no. 07-03-01074).

REFERENCES

1. Avgoropoulos, G., Ioannides, T., Papadopoulou, Ch., Baatista, J., Hocevar, S., and Matralis, H., *Catal. Today*, 2002, vol. 75, p. 157.
2. Avgoropoulos, G. and Ioannides, T., *Appl. Catal., A*, 2003, vol. 244, p. 155.
3. Kahlich, M.J., Gasteiger, H.A., and Behm, R.J., *J. Catal.*, 1997, vol. 171, p. 93.
4. Lee, S.J., Mukerjee, S., Ticinelli, E.A., and VcBreen, J., *Electrochim. Acta*, 1999, vol. 44, p. 3283.
5. Avgoropoulos, G., Ioannides, T., Matralis, H., Baatista, J., and Hocevar, S., *Catal. Lett.*, 2001, vol. 73, p. 33.
6. Igarashi, H., Uchida, H., Suzuki, M., and Watanabe, M., *Appl. Catal., A*, 1997, vol. 159, p. 159.
7. Ito, S.-I., Fujimori, T., Nagashima, K., Yuzaki, K., and Kumimori, K., *Catal. Today*, 2000, vol. 57, p. 247.
8. Cheng, W.H., *React. Kinet. Catal. Lett.*, 1996, vol. 58, p. 329.
9. Torres, R.M., Sachez, A., Ueda, K., Tanaka, K., and Haruta, M., *J. Catal.*, 1997, vol. 168, p. 125.
10. Liotta, L.F., Di CarioG., Pantaleo G., Deganello G., *Catal. Commun.*, 2005, vol. 6, p. 329.
11. Kang, M., Song, M.W., and Lee, C.H., *Appl. Catal., A*, 2003, vol. 251, no. 1, p. 143.
12. Tang, C.-W., Kuo, C.-C., Kuo, M.-C., Wang, C.-B., and Chien, S.-H., *Appl. Catal., A*, 2006, vol. 309, p. 37.
13. Natile, M.M. and Glisenti, A., *Chem. Mater.*, 2005, vol. 17, no. 14, p. 3403.
14. Liu, W. and Flytzani-Stefanopoulos, M., *J. Catal.*, 1995, vol. 153, p. 304.
15. Liu, W. and Flytzani-Stefanopoulos, M., *J. Catal.*, 1995, vol. 153, p. 317.
16. Sedmak, G., Hacevak, S., and Levec, J., *J. Catal.*, 2003, vol. 213, p. 135.
17. Ratnasamy, P., Srinavas, D., Satyanarayana, C.V.V., Manikandak, P., Kumaran, R.S.S., Sachin, M., and Shetti, V.N., *J. Catal.*, 2003, vol. 204, p. 455.
18. Marban, J. and Fuertes, A.B., *Appl. Catal., B*, 2005, vol. 57, no. 1, p. 34.
19. Il'ichev, A.N., Firsova, A.A., and Korchak, V.N., *Kinet. Katal.*, 2006, vol. 47, no. 4, p. 602 [*Kinet. Catal.* (Engl. Transl.), vol. 47, no. 4, p. 585].
20. Firsova, A.A., Il'ichev, A.N., Khomenko, T.I., Gorobinskii, L.V., Maksimov, Yu.V., Suzdalev, I.P., and Korchak, V.N., *Kinet. Katal.*, 2007, vol. 48, no. 2, p. 298 [*Kinet. Catal.* (Engl. Transl.), vol. 48, no. 2, p. 282].
21. Firsova, A.A., Khomenko, T.I., Il'ichev, A.N., and Korchak, V.N., *Kinet. Katal.*, 2008, vol. 49, no. 5, p. 713 [*Kinet. Catal.* (Engl. Transl.), vol. 49, no. 5, p. 682].
22. Dow, W.P. and Huang, T.J., *J. Catal.*, 1996, vol. 160, p. 171.
23. Kaputo, T., Pirone, R., and Russo, G., *Kinet. Katal.*, 2006, vol. 47, no. 5, p. 779 [*Kinet. Catal.* (Engl. Transl.), vol. 47, no. 5, p. 756].
24. Kuznetsova, T.G. and Sadykov, V.A., *Kinet. Katal.*, 2008, vol. 49, no. 6, p. 886 [*Kinet. Catal.* (Engl. Transl.), vol. 49, no. 6, p. 840].
25. Dow, W.-P., Wang, Y.-P., and Huang, T.-J., *J. Catal.*, 1996, vol. 160, p. 155.
26. Cobb, J.B.C., Bennet, A., Chinchen, G.C., Davies, L., Heaton, B.T., and Iggo, J.A., *J. Catal.*, 1996, vol. 164, p. 268.
27. Labaki, M., Lamon'e, Zh.-F., Siffert, S., Zhilinskaya, E.A., and Abukais, A., *Kinet. Katal.*, 2004, vol. 45, no. 2, p. 245 [*Kinet. Catal.* (Engl. Transl.), vol. 45, no. 2, p. 227].
28. Chernavskii, P.A., Lermontov, A.S., Pankina, G.V., Torbin, S.N., and Lunin, V.V., *Kinet. Katal.*, 2002, vol. 43, no. 2, p. 292 [*Kinet. Catal.* (Engl. Transl.), vol. 43, no. 2, p. 268].
29. Riva, R., Miessner, H., Vitali, R., and Del Piero, G., *Appl. Catal., A*, 2000, vol. 196, p. 111.

30. Fierro, G., Lo, Jacono, M., Inversi, M., Dragone, R., and Porta, P., *Top. Catal.*, 2000, vol. 10, p. 39.

31. Cotton, F.A. and Wilkinson, G., *Advanced Inorganic Chemistry*, New York: Wiley, 1966.

32. Davydov, A.A., *IK-spektroskopiya v khimii poverkhnosti okislov* (IR Spectroscopy Applied to the Chemistry of Oxide Surfaces), Novosibirsk: Nauka, 1984.

33. Tikhov, S.F., Sadykov, V.A., Kryukova, G.N., Paukshtis, E.A., et al., *J. Catal.*, 1992, vol. 134, p. 506.

34. Snytnikov, P.V., Stadnichenko, A.I., Semin, G.L., Belyaev, V.D., Boronin, A.I., and Sobyanin, V.A., *Kinet. Katal.*, 2007, vol. 48, no. 3, p. 463 [*Kinet. Catal.* (Engl. Transl.), vol. 48, no. 3, p. 439].

35. Manzoli, M., Monte, R.D., Boccuzzi, F., Colluccia, S., and Kaspar, J., *Appl. Catal., B*, 2005, vol. 61, p. 192.

36. Matyshak, V.A. and Krylov, O.V., *Kinet. Katal.*, 2002, vol. 43, no. 3, p. 442 [*Kinet. Catal.* (Engl. Transl.), vol. 43, no. 3, p. 391].

37. Krylov, O.V. and Matyshak, V.A., *Promezhutochnye soedineniya v geterogennom katalize* (Intermediate Compounds in Heterogeneous Catalysis), Moscow: Nauka, 1996.

38. Sedmak, G., Hocevar, S., and Levec, J., *J. Catal.*, 2003, vol. 213, p. 135.